chromophore ionization potential on speed and magnitude of photorefractive effects in poly-N-vinylcarbazole based polymer composites. *J. Chem. Phys.* **112,** 11030–11037 (2000).
26. Kippelen, B. *et al.* Infrared photorefractive polymers and their applications for imaging. *Science* **279,** 54–57 (1998).
27. Boppart, S. A. *et al. In vivo* cellular optical coherence tomography imaging. *Nature Med.* **4,** 861–865 (1998).
28. Hummelen, J. C. *et al.* Preparation and characterization of fulleroid and methanofullerene derivatives. *J. Org. Chem.* **60,** 532–538 (1995).

Acknowledgements

We thank R. Bittner, D. Müller, M. Hofmann and R. Birngruber for discussions. Financial support was granted by the Volkswagen Foundation (Germany), the European Space Agency (MAP-project), the Fonds der Chemischen Industrie (Germany), and the Bavarian government through 'Neue Werkstoffe' (Germany).

Competing interests statement

The authors declare that they have no competing financial interests.

Correspondence and requests for materials should be addressed to K.M. (e-mail: klaus.meerholz@uni-koeln.de).

Hydrogen from catalytic reforming of biomass-derived hydrocarbons in liquid water

R. D. Cortright, R. R. Davda & J. A. Dumesic

Department of Chemical Engineering, University of Wisconsin, Madison, Wisconsin 53706, USA

Concerns about the depletion of fossil fuel reserves and the pollution caused by continuously increasing energy demands make hydrogen an attractive alternative energy source. Hydrogen is currently derived from nonrenewable natural gas and petroleum[1], but could in principle be generated from renewable resources such as biomass or water. However, efficient hydrogen production from water remains difficult and technologies for generating hydrogen from biomass, such as enzymatic decomposition of sugars[2–5], steam-reforming of bio-oils[6–8] and gasification[9], suffer from low hydrogen production rates and/or complex processing requirements. Here we demonstrate that hydrogen can be produced from sugars and alcohols at temperatures near 500 K in a single-reactor aqueous-phase reforming process using a platinum-based catalyst. We are able to convert glucose—which makes up the major energy reserves in plants and animals—to hydrogen and gaseous alkanes, with hydrogen constituting 50% of the products. We find that the selectivity for hydrogen production increases when we use molecules that are more reduced than sugars, with ethylene glycol and methanol being almost completely converted into hydrogen and carbon dioxide. These findings suggest that catalytic aqueous-phase reforming might prove useful for the generation of hydrogen-rich fuel gas from carbohydrates extracted from renewable biomass and biomass waste streams.

We consider production of hydrogen by low-temperature reforming (at 500 K) of oxygenated hydrocarbons having a C:O stoichiometry of 1:1. For example, reforming of the sugar–alcohol sorbitol to H_2 and CO_2 occurs according to the following stoichiometric reaction:

$$C_6O_6H_{14}(l) + 6H_2O(l) \rightleftharpoons 13H_2(g) + 6CO_2(g) \quad (1)$$

The equilibrium constant for reaction (1) per mole of CO_2 is of the order of 10^8 at 500 K, indicating that the conversion of sorbitol in the presence of water to H_2 and CO_2 is highly favourable. However, the selective generation of hydrogen by this route is difficult because the products H_2 and CO_2 readily react at low temperatures to form alkanes and water. For example, the equilibrium constant at 500 K for the conversion of CO_2 and H_2 to methane (reaction 2) is of the order of 10^{10} per mole of CO_2.

$$CO_2(g) + 4H_2(g) \rightleftharpoons CH_4(g) + 2H_2O(g) \quad (2)$$

Figure 1 shows a schematic representation of the reaction pathways we believe to be involved in the formation of H_2 and alkanes from oxygenated hydrocarbons over a metal catalyst. The reactant undergoes dehydrogenation steps on the metal surface to give adsorbed intermediates before the cleavage of C–C or C–O bonds. With platinum, the catalyst we use, the activation energy barriers for cleavage of O–H and C–H bonds are similar[10]; however, Pt–C bonds are more stable than Pt–O bonds, so adsorbed species are probably bonded preferentially to the catalyst surface through Pt–C bonds. Subsequent cleavage of C–C bonds leads to the formation of CO and H_2, and CO reacts with water to form CO_2 and H_2 by the water–gas shift reaction (that is, $CO + H_2O \rightleftharpoons CO_2 + H_2$)[11,12].

The further reaction of CO and/or CO_2 with H_2 leads to alkanes and water by methanation and Fischer–Tropsch reactions[13–15]; this H_2 consuming reaction thus represents a series-selectivity challenge. In addition, undesirable alkanes can form on the catalyst surface by cleavage of C–O bonds, followed by hydrogenation of the resulting adsorbed species. This process constitutes a parallel-selectivity challenge. Another pathway that contributes to this parallel-selectivity challenge is cleavage of C–O bonds through dehydration reactions catalysed by acidic sites associated with the catalyst support[16,17] or catalysed by protons in the aqueous solution[18,19], followed by hydrogenation reactions on the catalyst. In addition, organic acids can be formed by dehydrogenation reactions catalysed by the metal, followed by rearrangement reactions[20] that take place in solution or on the catalyst. These organic acids lead to the formation of alkanes from carbon atoms that are not bonded to oxygen atoms.

Table 1 summarizes our experimental results for aqueous-phase reforming of glucose, the compound most relevant to hydrogen production from biomass, as well as for the reforming of sorbitol, glycerol, ethylene glycol and methanol. Reactions were carried out over a Pt/Al_2O_3 catalyst at 498 and 538 K (see Methods for experimental details). The fractions of the feed carbon detected in the effluent gas and liquid streams yield a complete carbon balance for all feed molecules, indicating that negligible amounts of carbon have been deposited on the catalyst. Catalyst performance was stable

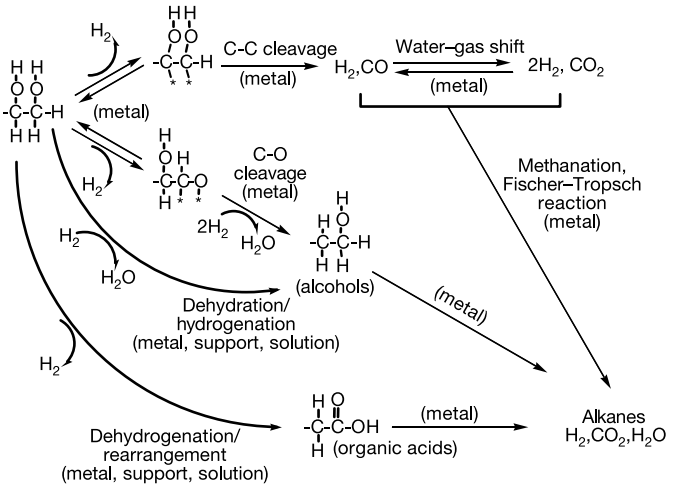

Figure 1 Reaction pathways for production of H_2 by reactions of oxygenated hydrocarbons with water. (Asterisk represents a surface metal site.)

for long periods of time on stream (for example, 1 week). Results from replicate runs agree to within ±3%.

The hydrogen selectivities shown in Table 1 are defined as the number of H_2 molecules detected in the effluent gas, normalized by the number of H_2 molecules that would be present if the carbon atoms detected in the effluent gas molecules had all participated in the reforming reaction. (That is, we infer the amount of converted glucose, sorbitol, glycerol, ethylene glycol and methanol from the carbon-containing gas-phase products and assume that each of the feed molecules would yield 2, 13/6, 7/3, 5/2 or 3 molecules of H_2, respectively.) Alkane selectivity is defined as the number of carbon atoms in the gaseous alkane products normalized by the total number of carbon atoms in the gaseous effluent stream.

Figure 2 illustrates that the selectivity for H_2 production improves in the order glucose < sorbitol < glycerol < ethylene glycol < methanol. Figure 2 also implies that lower operating temperatures result in higher H_2 selectivities, although this trend is in part due to the lower conversions achieved at lower temperatures. The selectivity for alkane production follows a trend with respect to reactant that is opposite to that exhibited by the H_2 selectivity.

The gas streams from aqueous-phase reforming of the oxygenated hydrocarbons were found to contain low levels of CO (that is, less than 300 p.p.m.). For aqueous-phase reforming of glycerol, where analysis of liquid-phase products is more tractable compared to sorbitol and glucose, the major reaction intermediates detected include (in approximate order of decreasing concentration) ethanol, 1,2-propanediol, methanol, 1-propanol, acetic acid, ethylene glycol, acetol, 2-propanol, propionic acid, acetone, propionaldehyde, and lactic acid. Analysis of the gas phase effluent indicates the presence of trace amounts of methanol and ethanol (about 300 p.p.m.).

High hydrogen yields are only obtained when using sorbitol, glycerol and ethylene glycol as feed molecules for aqueous-phase reforming. Although these molecules can be derived from renewable feedstocks[21–24], the reforming of less reduced and more immediately available compounds such as glucose is likely to be more practical; but hydrogen yields for glucose reforming are relatively low (Table 1 and Fig. 2). However, we expect that improvements in catalyst performance, reactor design, and reaction conditions may increase the hydrogen selectivity for the direct aqueous-phase reforming of sugars. For example, the lower H_2 selectivities for the aqueous-phase reforming of glucose, compared to that achieved using the other oxygenated hydrocarbon reactants, are caused at least partially by homogeneous reactions of glucose in the aqueous phase at the temperatures used in this study[19]. Thus, higher selectivities for H_2 from aqueous-phase reforming of glucose might be achieved by reactor designs that maximize the number of catalytically active sites (leading to desirable surface reactions) and minimize the void volume (leading to undesirable liquid-phase reactions) in the reactor.

Here, using Pt/Al_2O_3 as catalyst, we found that lower glucose concentrations correlated with higher selectivities for hydrogen production, and reforming experiments were therefore conducted at low feed concentrations of 1 wt%, which corresponds to a molar ratio H_2O/C_1 of 165. Processing such dilute solutions is economically not practical, even though reasonably high hydrogen yields are achieved (Table 1). However, undesirable homogeneous reactions, as observed with glucose, pose less of a problem when using sorbitol, glycerol, ethylene glycol and methanol, which makes it possible to generate high yields of hydrogen by the aqueous-phase reforming of more concentrated solutions containing these compounds. For example, we have found that upon increasing the feed concentrations of ethylene glycol or glycerol to 10 wt% (molar ratio $H_2O/C_1 = 15$), it is still possible to achieve high conversions and high selectivities for H_2 production. (A hydrogen selectivity of 97% was achieved with 62% conversion of 10 wt% ethylene glycol; and a hydrogen selectivity of 70% was achieved with 77% conversion of 10 wt% glycerol.) A molar H_2O/C_1 ratio of 15 is still higher than that typically utilized in conventional vapour-phase reforming of hydrocarbons (molar $H_2O/C_1 = 3$ to 5); but our aqueous-phase reforming system has the advantage of not requiring energy-intensive vaporization of water to generate steam.

Operating at higher reactant concentrations and lower conversion levels leads to higher rates of hydrogen production. Rates of hydrogen production are measured as turnover frequencies (that is, rates normalized by the number of surface metal atoms as determined from the irreversible uptake of CO at 300 K). For example, the turnover frequency for production of hydrogen at 498 K from a 1 wt% ethylene glycol solution is 0.08 min^{-1} for the 90% conversion run listed in Table 1 (weight-hourly space velocity, WHSV = 0.008 g of ethylene glycol per g of catalyst per h), but increases to 0.7 min^{-1} for a feed containing 10 wt% ethylene glycol (run at 498 K and at a higher WHSV of 0.12 g of ethylene glycol per g of catalyst per h). The hydrogen selectivity for this latter run is equal to 97% at a conversion of 62%. The turnover frequency for hydrogen production from 10 wt% ethylene glycol at 498 K increased further to 7 min^{-1} when higher space-velocities were used (WHSV = 18 g of ethylene glycol per g of catalyst per h) with a highly dispersed 3 wt% Pt/Al_2O_3 catalyst consisting of smaller alumina particles (63–125 μm) to minimize transport limitations. The hydrogen selectivity for this kinetically controlled run was 99% at a conversion of 3.5%.

The rates of formation of H_2 from aqueous-phase reforming of 10 wt% glucose, sorbitol, glycerol, ethylene glycol and methanol at 498 K over a 3 wt% Pt/Al_2O_3 catalyst under conditions to minimize transport limitations and at low conversions of the reactant have

Table 1 **Experimental data for reforming of oxygenated hydrocarbons**

	Glucose		Sorbitol		Glycerol		Ethylene glycol		Methanol	
Temperature (K)	498	538	498	538	498	538	498	538	498	538
Pressure (bar)	29	56	29	56	29	56	29	56	29	56
% Carbon in liquid-phase effluent	51	15	39	12	17	2.8	11	2.9	6.5	6.4
% Carbon in gas-phase effluent	50	84	61	90	83	99	90	99	94	94
Gas-phase composition										
H_2 (mol. %)	51	46	61	54	64.8	57	70	68.7	74.6	74.8
CO_2 (mol. %)	43	42	35	36	29.7	32	29.1	29	25	24.6
CH_4 (mol. %)	4.0	7.0	2.5	6.0	4.2	8.3	0.8	2.0	0.4	0.6
C_2H_6 (mol. %)	2.0	2.7	0.7	2.3	0.9	2.0	0.1	0.3	0.0	0.0
C_3H_8 (mol. %)	0.0	1.0	0.8	1.0	0.4	0.7	0.0	0.0	0.0	0.0
C_4, C_5, C_6 alkanes (mol. %)	0.0	1.2	0.0	0.6	0.0	0.0	0.0	0.0	0.0	0.0
% H_2 selectivity*	50	36	66	46	75	51	96	88	99	99
% Alkane selectivity†	14	33	15	32	19	31	4	8	1.7	2.7

The catalyst was loaded in a tubular reactor, housed in a furnace, and reduced prior to reaction kinetics studies. The reactor system was pressurized with N_2, and the reforming reaction was carried out at the listed reaction conditions. Each reaction condition was run for 24 h, during which the experimental data were collected. Further experimental details are provided in the Methods.

*% H_2 selectivity = (molecules H_2 produced/C atoms in gas phase)(1/RR) × 100, where RR is the H_2/CO_2 reforming ratio, which depends on the reactant compound. RR values for the compounds are: glucose, 2; sorbitol, 13/6; glycerol, 7/3; ethylene glycol, 5/2; methanol, 3. We note that H_2 and alkane selectivities do not add up to 100%, because they are based independently on H-balances and C-balances, respectively. % Carbon in gas and liquid phase effluents add to 100% for a complete carbon balance. Slight ± deviations from 100% are caused by experimental error.

†% Alkane selectivity = (C atoms in gaseous alkanes/total C atoms in gas phase product) × 100.

been measured to be 0.5, 1.0, 3.5, 7.0 and 7.0 min^{-1}, respectively. These turnover frequencies correspond to hydrogen production rates of 50, 100, 350, 700, and 700 l of H_2 (at standard temperature and pressure, 273 K and 1.01 bar) per l of reactor volume per h for each feed molecule, respectively. These rates compare favourably to the maximum rate of hydrogen production from glucose of about 5×10^{-3} l of H_2 per l of reactor volume per hour by enzymatic routes[5]. Normalization of the rates by the mass of catalyst used yields rates of about 3×10^3, 6×10^3, 2×10^4, 4×10^4, and 4×10^4 $\mu mol\, g^{-1}\, h^{-1}$ for hydrogen production at 498 K, from 10 wt% glucose, sorbitol, glycerol, ethylene glycol and methanol, respectively. These rates can be compared to the maximum value of 7×10^2 $\mu mol\, g^{-1}\, h^{-1}$ reported for hydrogen production from glucose by enzymatic routes. (For this comparison, we have assumed a typical value of 100 units per mg of protein, where a unit of enzyme activity corresponds to the amount of enzyme which under standard assay conditions converts 1 μmol of substrate per min).

If the hydrogen produced were fed to a fuel cell operating at 50% efficiency, the rate of hydrogen production in our reformer would generate approximately 1 kW of power per l of reactor volume. Electrical power might thus be generated cost-effectively by an integrated fuel-cell/liquid-phase reformer system fed with a low-cost carbohydrate stream derived from waste biomass (for example, corn stover, wheat straw, wood waste). The practical use of aqueous-phase reforming reactions in this manner would depend on efficient feed recycling strategies and on efficient separation of hydrogen from the gaseous effluent stream. The gaseous effluents separated from the main product hydrogen could be combusted to generate the energy necessary for the liquid-phase-reforming reactor. However, some fuel cell applications might not require extensive purification because the main components in the reformer gas effluent other than hydrogen are CO_2 and methane, which can act as diluents[25]. Alcohols and organic acids are also present in the gas effluent, but only at trace levels (300 p.p.m. and about 5 p.p.m., respectively) which may not lead to irreversible poisoning[26].

Reforming reactions between hydrocarbons and water to generate hydrogen are endothermic, and conventional steam-reforming of petroleum thus depends on the combustion of additional hydrocarbons to provide the heat needed to drive the reforming reaction. In contrast, the energy required for the aqueous-phase reforming of oxygenated hydrocarbons may be produced internally, by allowing a fraction of the oxygenated compound to form alkanes through exothermic reaction pathways. In this respect, the formation of a mixture of hydrogen and alkanes from aqueous-phase reforming of glucose, as accomplished in the present study, is essentially neutral energetically, and little additional energy is required to drive the reaction. In fact, the energy contained in these alkanes could be used as a feed to an internal combustion engine or suitable fuel cell; this would allow the use of biomass-derived energy to drive the aqueous-phase reforming of glucose (and biomass more generally) with high yields to renewable energy.

While the present findings establish that Pt-based catalysts show high activities and good selectivity for the production of hydrogen from sugars and alcohols by aqueous-phase reforming reactions, improvements are necessary to render the process useful. Highly active catalytic materials that can satisfy the series and parallel selectivity challenges outlined in Fig. 1, but at a lower materials cost than for Pt, are particularly desirable. Moreover, new combinations of catalysts and reactor configurations are needed to obtain higher hydrogen yields from more concentrated solutions of glucose, given that glucose is the only compound we have tested that is directly relevant to biomass utilization. We believe that such improvements are possible, for example, by searching for catalysts that exhibit higher activity at lower temperatures, to minimize the deleterious effects of homogeneous decomposition reactions. □

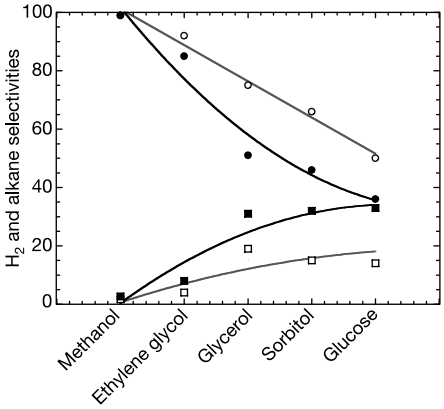

Figure 2 Selectivities (%) versus oxygenated hydrocarbon. H_2 selectivity (circles) and alkane selectivity (squares) from aqueous-phase reforming of 1 wt% oxygenated hydrocarbons over 3 wt% Pt/Al_2O_3 at 498 K (open symbols) and 538 K (filled symbols). The aqueous feed solution was fed to the reactor at a weight-hourly space velocity of 0.008 g of oxygenated hydrocarbon per gram of catalyst per hour. High conversions of the reactant were achieved under these conditions (50–99% conversion to gas-phase carbon, as indicated in Table 1) to provide a rigorous test of the carbon mass balance.

Methods

Experiments for the aqueous-phase reforming of glucose, sorbitol, glycerol, ethylene glycol and methanol were performed over a 3 wt% Pt catalyst supported on nanofibres of γ-alumina (500 $m^2\, g^{-1}$, Argonide Corp.). The catalyst was prepared by incipient wetness impregnation of alumina with tetraamine platinum nitrate solution, followed by drying at 380 K, calcination at 533 K in flowing oxygen and reduction at 533 K in flowing hydrogen. Chemisorption experiments using carbon monoxide at 300 K showed a CO uptake of 105 μmol per g of catalyst. A stainless steel tubular reactor (having an inner diameter of 5 mm and length of 45 cm) was loaded with 4.5 g of the pelletized Pt/Al_2O_3 catalyst, which was then reduced under flowing hydrogen at 533 K. The total pressure of the system was then increased by addition of nitrogen to a value slightly higher than the vapour pressure of water at the reaction temperature. The system pressure was controlled by a backpressure regulator. An aqueous solution containing 1 wt% of the oxygenated compound was fed continuously, using a high-performance liquid chromatography (HPLC) pump, at 3.6 ml h^{-1} into the reactor heated to the desired reaction temperature. Under these conditions, the WHSV was 0.008 g of oxygenated compound per g of catalyst per h through the reactor. The effluent from the reactor was water-cooled in a double-pipe heat exchanger to liquefy the condensable vapours. The fluid from this cooler was combined with the nitrogen make-up gas at the top of the cooler, and the gas and liquid were separated in a stainless-steel vessel (about 130 cm^3) maintained at the system pressure. The effluent liquid was drained periodically (every 12 h) for total organic carbon (TOC) analysis and for detection of the primary carbonaceous species using gas chromatography and HPLC. The effluent gas stream passed through the back-pressure regulator and was analysed with several online gas chromatographs. The kinetic data for each reaction condition were typically collected over a 24-h period, after which the reaction conditions were changed. The catalyst performance was stable for times on stream of at least 1 week.

Received 6 February; accepted 23 July 2002; doi:10.1038/nature01009.

1. Rostrup-Nielsen, J. Conversion of hydrocarbons and alcohols for fuel cells. *Phys. Chem. Chem. Phys.* **3,** 283–288 (2001).
2. Kumar, N. & Das, D. Enhancement of hydrogen production by enterobacter cloacae IIT-BT 08. *Process Biochem.* **35,** 589–593 (2000).
3. Woodward, J. *et al.* Enzymatic hydrogen production: Conversion of renewable resources for energy production. *Energy Fuels* **14,** 197–201 (2000).
4. Yokoi, H. *et al.* Microbial hydrogen production from sweet potato starch residue. *J. Biosci. Bioeng.* **91,** 58–63 (2001).
5. Woodward, J., Orr, M., Cordray, K. & Greenbaum, E. Enzymatic production of biohydrogen. *Nature* **405,** 1014 (2000).
6. Garcia, L., French, R., Czernik, S. & Chornet, E. Catalytic steam reforming of bio-oils for the production of hydrogen: Effects of catalyst composition. *Appl. Catal. A* **201,** 225–239 (2000).
7. Amphlett, J. C., Leclerc, S., Mann, R. F., Peppley, B. A. & Roberge, P. R. Fuel cell hydrogen production by catalytic ethanol-steam reforming. *Proc. 33rd Intersoc. Energy Convers. Eng. Conf.* **269,** 1–7 (1998).
8. Marquevich, M., Czernik, S., Chornet, E. & Montane, D. Hydrogen from biomass: Steam reforming of model compounds of fast-pyrolysis oil. *Energy Fuels* **13,** 1160–1166 (1999).
9. Milne, T. A., Elam, C. C. & Evans, R. J. *Hydrogen from Biomass: State of the Art and Research Challenges* 1–82 (National Renewable Energy Laboratory, Golden, CO, 2002).
10. Greeley, J. & Mavrikakis, M. A first-principles study of methanol decomposition on Pt(111). *J. Am. Chem. Soc.* **124,** 7193–7201 (2002).
11. Grenoble, D. C., Estadt, M. M. & Ollis, D. F. The chemistry and catalysis of the water gas shift reaction. 1. The kinetics over supported metal catalysts. *J. Catal.* **67,** 90–102 (1981).
12. Hilaire, S., Wang, X., Luo, T., Gorte, R. J. & Wagner, J. A comparative study of water-gas shift reaction over ceria supported metallic catalysts. *Appl. Catal. A* **215,** 271–278 (2001).
13. Iglesia, E., Soled, S. L. & Fiato, R. A. Fischer-Tropsch synthesis on cobalt and ruthenium. Metal

dispersion and support effects on reaction rate and selectivity. *J. Catal.* **137,** 212–224 (1992).
14. Kellner, C. S. & Bell, A. T. The kinetics and mechanism of carbon monoxide hydrogenation over alumina-supported ruthenium. *J. Catal.* **70,** 418–432 (1981).
15. Vannice, M. A. The catalytic synthesis of hydrocarbons from H_2/CO mixtures over the group VIII metals V. The catalytic behaviour of silica-supported metals. *J. Catal.* **50,** 228–236 (1977).
16. Bates, S. P. & Van Santen, R. A. Molecular basis of zerolite catalysis: A review of theoretical simulations. *Adv. Catal.* **42,** 1–114 (1998).
17. Gates, B. *Catalytic Chemistry* (Wiley, New York, 1992).
18. Eggleston, G. & Vercellotti, J. R. Degradation of sucrose, glucose and fructose in concentrated aqueous solutions under constant pH conditions at elevated temperature. *J. Carbohydr. Chem.* **19,** 1305–1318 (2000).
19. Kabyemela, B. M., Adschiri, T., Malaluan, R. M. & Arai, K. Glucose and fructose decomposition in subcritical and supercritical water: Detailed reaction pathway, mechanisms, and kinetics. *Ind. Eng. Chem. Res.* **38,** 2888–2895 (1999).
20. Collins, P. & Ferrier, R. *Monosaccharides: Their Chemistry and Their Roles in Natural Products* (Wiley, West Sussex, England, 1995).
21. Li, H., Wang, W. & Deng, J. F. Glucose hydrogeneration to sorbitol over a skeletal Ni-P amorphous alloy catalyst (Raney Ni-P). *J. Catal.* **191,** 257–260 (2000).
22. Blanc, B., Bourrel, A., Gallezot, P., Haas, T. & Taylor, P. Starch-derived polyols for polymer technologies: Preparation by hydrogenolysis on metal catalysts. *Green Chem.* **2,** 89–91 (2000).
23. Narayan, R., Durrence, G. & Tsao, G. T. Ethylene glycol and other monomeric polyols from biomass. *Biotechnol. Bioeng. Symp.* **14,** 563–571 (1984).
24. Tronconi, E. *et al.* A mathematical model for the catalytic hydrogenolysis of carbohydrates. *Chem. Eng. Sci.* **47,** 2451–2456 (1992).
25. Larminie, J. & Dicks, A. *Fuel Cell Systems Explained* 189 (Wiley, West Sussex, England, 2000).
26. Amphlett, J. C., Mann, R. F. & Peppley, B. A. On board hydrogen purification for steam reformer/PEM fuel cell vehicle power plants. *Hydrogen Energy Prog. X, Proc. 10th World Hydrogen Energy Conf.* **3,** 1681–1690 (1998).

Acknowledgements

We thank K. Allen, J. Shabaker and G. Huber for assistance in reaction kinetics measurements. We also thank G. Huber for help with catalyst preparation/characterization and for TOC analyses, and M. Sanchez-Castillo for assistance with analysis of reaction products. We thank M. Mavrikakis and researchers at Haldor Topsøe A/S for reviews and discussion. This work was supported by the US Department of Energy (DOE), Office of Basic Energy Sciences, Chemical Science Division.

Competing interests statement

The authors declare competing financial interests: details accompany the paper on *Nature*'s website (http://www.nature.com/nature).

Correspondence and requests for materials should be addressed to J.A.D. (e-mail: dumesic@engr.wisc.edu).

Pfiesteria shumwayae kills fish by micropredation not exotoxin secretion

Wolfgang K. Vogelbein*, Vincent J. Lovko*†, Jeffrey D. Shields*†, Kimberly S. Reece*, Patrice L. Mason*, Leonard W. Haas* & Calvin C. Walker‡

* *Virginia Institute of Marine Science, The College of William and Mary, Gloucester Point, Virginia 23062, USA*
‡ *United States Environmental Protection Agency, National Health and Environmental Effects Research Laboratory, Gulf Ecology Division, 1 Sabine Island Drive, Gulf Breeze, Florida 32561, USA*
† *These authors contributed equally to this work*

***Pfiesteria piscicida* and *P. shumwayae* reportedly secrete potent exotoxins thought to cause fish lesion events, acute fish kills and human disease in mid-Atlantic USA estuaries[1–7]. However, *Pfiesteria* toxins have never been isolated or characterized[8]. We investigated mechanisms by which *P. shumwayae* kills fish using three different approaches. Here we show that larval fish bioassays conducted in tissue culture plates fitted with polycarbonate membrane inserts exhibited mortality (100%) only in treatments where fish and dinospores were in physical contact. No mortalities occurred in treatments where the membrane prevented contact between dinospores and fish. Using differential centrifugation and filtration of water from a fish-killing culture, we produced 'dinoflagellate', 'bacteria' and 'cell-free' fractions. Larval fish bioassays of these fractions resulted in mortalities (60–100% in less than 24 h) only in fractions containing live dinospores ('whole water', 'dinoflagellate'), with no mortalities in 'cell-free' or 'bacteria'-enriched fractions. Videomicrography and electron microscopy show dinospores swarming toward and attaching to skin, actively feeding, and rapidly denuding fish of epidermis. We show here that our cultures of actively fish-killing *P. shumwayae* do not secrete potent exotoxins; rather, fish mortality results from micropredatory feeding.**

Massive fish kills in mid-Atlantic USA estuaries involving several million Atlantic menhaden, *Brevoortia tyrannus*, have been attributed to dinoflagellates of the toxic *Pfiesteria* complex (TPC)[9]. Potent ichthyotoxins secreted during *Pfiesteria* blooms are thought to be responsible for mortality as well as for deeply penetrating, so-called '*Pfiesteria*-specific' skin ulcers in these fish[1,5,9]. However, earlier investigations attributed the menhaden ulcers to fungal infections[10,11], and *Aphanomyces invadans*, a highly pathogenic oomycete[12], is now considered the aetiologic agent[13,14]. We recently demonstrated that *A. invadans* is a primary pathogen, able to elicit menhaden ulcer disease in the absence of *Pfiesteria* species or other environmental stressors[15]. Thus, the role of *Pfiesteria* species in menhaden lesion events is now questioned[13–16].

In contrast to the oomycete-induced ulcers of wild menhaden, laboratory exposure of fishes to an unidentified *Pfiesteria* species elicited rapid, widespread epidermal erosion, osmoregulatory dysfunction and death, with potent exotoxins assumed responsible[4]. However, direct attachment of *P. shumwayae* dinospores to skin, gills, olfactory organs, the oral mucosa and the lateral line canal, associated with extensive tissue damage, has been observed[16]. A direct physical association with these fish tissues had not to our knowledge been previously reported, and this suggested an alternative mechanism of pathogenesis for *P. shumwayae*. To better understand this association and to clarify the consequences of dinospore attachment, we conducted laboratory challenges using a sensitive larval fish bioassay.

We exposed larval sheepshead minnows, *Cyprinodon variegatus*, to *Pfiesteria* spp. in six-well tissue culture plates containing polycarbonate membrane inserts (Millicell). This created two compartments within each well ('in', inside insert; 'out', outside insert), allowing separation of fish from dinospores across a permeable membrane (Fig. 1). Mortalities occurred only in treatments where fish and *P. shumwayae* dinospores were in direct physical contact (Fig. 2a: B in, D in, F). Fish physically separated from dinospores (A in, B out versus in) did not die, even if they resided within the same well as dying fish in contact with dinospores (B in versus out). Fish in negative controls (C) and fish exposed to a non-pathogenic strain

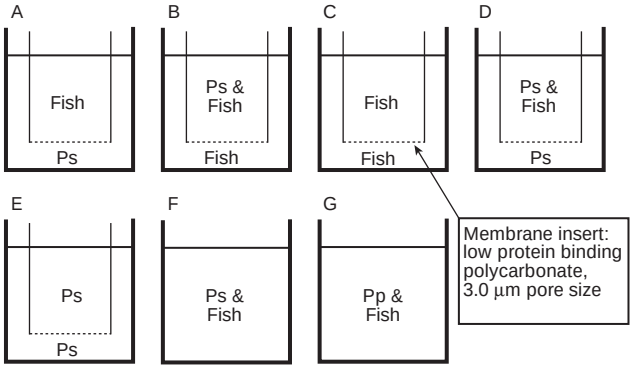

Figure 1 Experimental design for the membrane insert study using larval *Cyprinodon variegatus* exposed to *Pfiesteria shumwayae* (Ps) and *P. piscicida* (Pp).